Desalination and Water Treatment
www.deswater.com
doi: 10.1080/19443994.2013.862033

52 (2014) 5068–5075
July

Taylor & Francis
Taylor & Francis Group

Dye effluent treatment using PVDF UF membranes with different properties

Xiao-rong Meng[a]*, Nan Zhang[a], Xu-dong Wang[b], Lei Wang[b], Dan-xi Huang[b] Rui Miao[b]

[a]*School of Science, Xi'an University of Architecture and Technology, Xi'an 710055, China*
Tel. +86 13152171015; email: mxr5@163.com
[b]*School of Environmental & Municipal Engineering, Xi'an University of Architecture and Technology, Xi'an 710055, China*

Received 14 May 2013; Accepted 6 October 2013

ABSTRACT

Using DMAc as solvent, water as non-solvent, modified poly (vinylidene fluoride) (PVDF) ultrafiltration membranes (PSi, PA, PS) were prepared by precipitation phase inversion, blending with nano-silica (SiO_2), polyvinyl alcohol (PVA), and styrene maleic anhydride. The physical-chemical properties and morphology of PVDF membranes were characterized by FT-IR, water contact angle (WCA), swelling index, scanning electron microscopy, atomic force microscopy, etc. Considering reactive black 5 and congo red as the representatives of dye effluent pollutions, the filtration behavior to dye wastewater of four different types of PVDF UF membranes was discussed. Experimental results showed that, compared with original PVDF UF membrane, for three kinds of modified membrane, the first bubble pressure and strength (S) fell off to a certain extent, and the membrane surface roughness increased. Additionally, the cross-sectional macroporous and pure water flux (J) all increased. Especially, owing to the addition of PVA and SiO_2, the WCA and the adsorption amount (Q) of PA and PSi membranes were reduced extraordinarily, and flux recovery rate increased obviously. As a result, the hydrophilicity of PVDF membrane was improved significantly. Moreover, the rejection (r) to two dyes was also remained well, which showed a better anti-fouling ability.

Keywords: PVDF ultrafiltration; Modified membrane; dye effluent; membrane fouling

1. Introduction

The dye wastewater contains color and pollutants mainly formed by natural organic matter and synthetic organic compounds. Because of different fiber fabric of the dye used in printing and dye process, there were many traditional methods for dye wastewater treatment. However, membrane separation technology has been widely used in the field of dye wastewater treatment owing to its high separation efficiency and relatively simple process [1].

As reported, reverse osmosis (RO) and nanofiltration (NF) membranes were the first to be used in the membrane process of the treatment of dye wastewater. The applicability of RO membranes was limited by high osmotic pressure. RO membrane filtration has problem with fouling, which result in low fluxes and poor separation efficiency [2,3]. NF was proven to be

*Corresponding author.

Presented at the Conference on Water Resources and Urbanization Development, 26–27 September 2012, Tianjin, China

an ideal method for the pretreatment of highly concentrated and complex solutions [4]. However, NF separation was not very efficient, and NF operation pressure was a little bit higher than UF. In view of these abovementioned problems, ultrafiltration (UF) technology of low-pressure operation has entered into the stage of the dye wastewater treatment research. Han et al. [5]. prepared a copoly (phthalazinone biphenyl ether sulfone) (PPBES) UF membrane with a low molecular weight cut-off, and it was suitable to be utilized in dye wastewater treatment. Srivatava et al. [6] reported the performance of a modified poly(vinylidene fluoride) membrane for textile wastewater UF, obtained lower membrane fouling for separation and purification of dye solutions. On this basis, a UF membrane was confirmed by studies on removal of color and turbidity of dye effluent [7].

The same as the other processes of membrane treatment, membrane fouling has also become the bottleneck problem of the membrane treatment technology in the treatment of dye wastewater [8]. Some point of views support that the degree of membrane fouling is small when the charged dye molecules are the same as the electrification of the membrane surface, and the hydrophilic surface of the membrane will decrease the irreversible adsorption of contaminants on the membrane surface. When membrane materials have polar and dissociated functional groups, after contacting with the solution, because of the solvate and dissociation, the membrane surface will be charged [9].

Therefore, this study took inorganic nano-silica (SiO_2), hydrophilic polymer polyvinyl alcohol (PVA), and styrene maleic anhydride (SMA) copolymer with anhydride functional groups into the PVDF UF membrane, and examined the effect of the nature of the membrane materials and membrane structure on characteristics of membrane fouling behavior in the process of wastewater treatment. In dye wastewater removal, low-pressure UF is a meaningful reference.

2. Experimental

2.1. Materials

Poly(vinylidene fluoride) (PVDF, Solef, 6,020, $M_W \approx 573{,}000$ Da, density = 1.76×10^3 kg/m^3) was received from Belgian Solvay. Poly(vinylalcohol) (PVA, 18–99) was purchased from Sigma Company. Poly(ethylene glycol) (PEG, $M_W = 400$) was purchased from Guangdong Guanghua Sci-Tech Co., Ltd. SMA was purchased from Polyscope Company. Silicon dioxide (SiO_2, NB, 99.99%) was received from Shanghai. Reactive black 5 (RB5) ($M_W = 991.8$) and Congo red (CR) ($M_W = 696.7$) were obtained from Zhejiang. The molecular structures of both dyes are shown in Fig. 1.

2.2. Preparation of the UF membrane

The preparation method of PVDF UF membranes is described in the literature [10]. The composition of casting solution and membrane numbers are shown in Table 1. The cast solution was cast onto a glass plate to form a liquid film with the thickness of 200 μm. After 5 s exposure to air, the plate was immersed into a deionized water bath at 40℃.

2.3. Membrane characterization

2.3.1. Membrane morphology

Scanning electron microscope (SEM, JSM5800, Japan, JEOL) was used to inspect the cross-section and surface of the membranes. The membranes pieces were immersed in liquid nitrogen for freezing. And then the frozen membrane segments were kept in air for drying. The dried samples were gold sputtered for producing electric conductivity [11].

The surface roughness of membranes was analyzed by atomic force microscopy (AFM, DME model C-21, Denmark), the test condition are as in [12].

2.3.2. The properties of UF membrane

The chemical composition of the UF membrane was measured by FT-IR. Before testing, the film samples were required to dry in the 50℃ vacuum oven. (Test parameters: scan the wavelength range 4,000 to 400 cm^{-1}, the scanning precision 4 cm^{-1}, room temperature (25 ± 1℃), humidity 15%).

Water contact angle (WCA) was measured using the VCA-Optima (AST products, Inc, MA, USA). Five microlitre of distilled water was dropped on the membrane surface from a microsyringe with a stainless steel needle at room temperature (25 ± 1℃). WCA value was obtained for both top and bottom surface of each membrane sample and the time was kept 30 s [13].

The dry film was immersed in deionized water at 25℃ for 24 h. Then, the films were taken out from the water and wiped with filter paper. Wet weight was defined after soaking. The degree of swelling (SI) can be calculated:

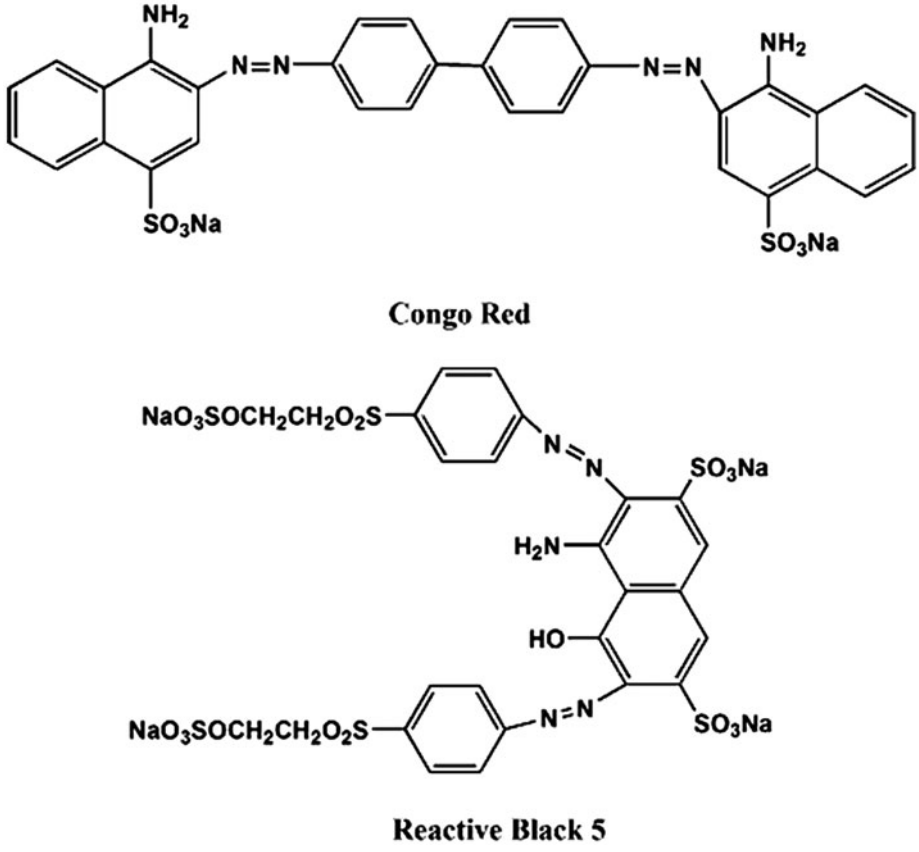

Fig. 1. Molecular structure of CR and RB5.

Table 1
The compositions of different casting solution and membrane numbers

Membrane	PVDF (%)	PEG (%)	PVA (%)	SiO_2 (%)	SMA (%)	LiCl (%)	DMAc (%)
P	17	3	0	0	0	3	77
PA	17	0	3	0	0	3	77
PSi	17	0	0	0	3	3	77
PS	17	0	0	3	0	3	77

$$SI = \frac{M_S - M_D}{M_S} \times 100\% \quad (1)$$

where M_S is the weight of the wet membrane (g), M_D is the weight of the dry membrane (g).

The mechanical strength of the membrane was measured by electronic single yarn tensile strength tester (HD021NS) samples with width of 1 cm, length of 15 cm, the folder distance was 100 mm, and the tensile speed was 100 mm/min. The test parameters are as in [14].

2.3.3. Structure parameters of the membrane

Structural parameters: Porosity of the membrane (ε) was measured by wet and dry membrane weight method [15].

$$\varepsilon = \frac{M_W - M_D}{\rho_w Al} \times 100\% \quad (2)$$

where M_W, M_D are the wet and dry membrane weight (g), respectively, A is the membrane area (cm^2), l is the average thickness (cm), ρ_w is the density of water (g/cm^3).

A flow-rate method was used to determine the pore size [16].

$$r_m = \sqrt{\frac{(2.9 - 1.75\varepsilon)8\eta l J}{\varepsilon A \Delta P}} \quad (3)$$

where ε is porosity, η is viscosity of water (Pa·S), l is the average thickness (cm), ΔP is transmembrane pressure (MPa), A is effective membrane area (cm^2), and J is the flux of pure water ($L\,m^{-2}\,h^{-1}$).

The first bubble pressure (FBP) of the membrane was measured by an automatic filter integrity tester (FJLGUARD-311) using ethanol as medium [17].

2.3.4. Permeability experiment

The water permeability and anti-fouling property of the membranes were evaluated in a dead-end stirred cell filtration system (Fig. 2). The sample membrane disk was precisely installed in a stirred dead-end cell with the transmembrane pressure was 0.1 MPa. All experiments were conducted at room temperature (25 ± 1°C). The pure water flux was calculated by Eq. (4):

$$J_P = \frac{Q}{A\Delta T} \quad (4)$$

where J_P is pure water flux ($L\,m^{-2}\,h^{-1}$), Q is the volume of permeated water (L), A is effective membrane area (m^2), and ΔT is the permeation time (h).

2.4. The filtration of dye wastewater and membrane fouling

2.4.1. Static adsorption

The membrane piece (4 cm × 5 cm) was placed into 50 mL of dye solution with the concentration of 50 mg/L, then the absorbance of the solution was determined at 488 nm and 598 nm after 24 h, respectively. Static adsorption amount was calculated by the Eq. (5):

$$Q = \frac{V(C_0 - C)}{S} \quad (5)$$

where Q (mg/cm^2) is static adsorption amount, V (mL) is the volume of dye solution, C_0 (mg/mL) the initial concentration of the solution, C (mg/mL) is dye solution concentration after the membrane adsorption, and S (cm^2) is the membrane area.

2.4.2. Treatment of dye effluent

The synthetic RB5 and CR dye solutions were prepared separately in 50 mg/L concentration. The synthetic dye solutions were passed through PA, PS and PSi membranes in a dead-end UF stirred cell at 50 TMP and the flux was calculated using Eq. (6) every half hour. The concentration of dyes in the dye solution and permeate was analyzed using the UV-spectrophotometer, at 595, 495 nm for RB5, CR dyes, respectively. The rejection of dye was evaluated using Eq. (6):

$$R = \left(1 - \frac{C_f}{C_p}\right) \times 100\% \quad (6)$$

where C_f and C_P are feed and permeate concentrations of the dye solutions, respectively.

2.4.3. The properties of membrane anti-fouling

Two processes were used in order to estimate the antifouling property of modified PVDF UF membranes

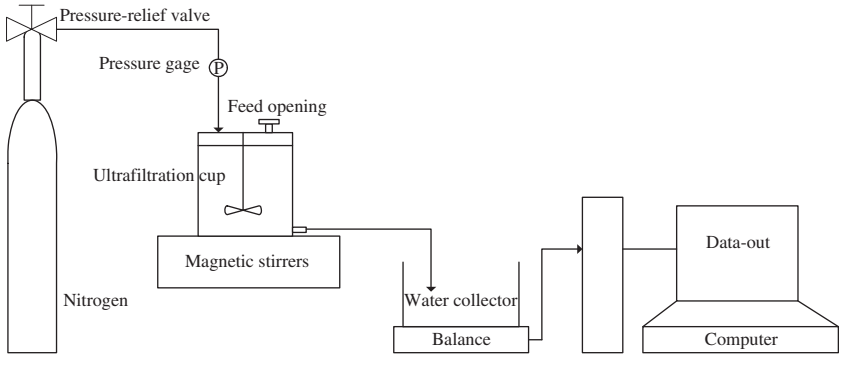

Fig. 2. Dead-end stirred cell filtration system.

in respect to RB5 and CR dye solutions. Before two processes, the steady-state water flux (J_{ws}) of the membrane was measured. For the first phase, the UF cell was empty, the membranes were cleaned with water and pure water flux in the first run was measured for 2.5 h. The membrane was rinsed with water after the first run was performed to remove trace amounts of dye adsorbed on the membrane. In the second phase, the same procedure was followed with the CR dye solution. The permeate flux of the CR dye solution in the second run (J_{wf}) and pure water flux in the second run were measured. Flux recovery (FR) was calculated using Eq. (7):

$$\mathrm{FR} = \left(\frac{J_{wf}}{J_{ws}}\right) \times 100\% \tag{7}$$

3. Results and discussion

3.1. Chemical composition of different PVDF membranes

Fig. 3 shows the FT-IR spectra of P, PA, PS, and PSi. Compared with the spectra of P, the characterized absorption of Si-O-Si at 1,103 and 798 cm^{-1}, the characterized absorption of the benzene ring between 700–900 cm^{-1} and anhydride at 1,820 and 1,760 cm^{-1} existed in the PS membrane. Therefore, these indicated that a certain amount of additives remained in blend membranes. It can be also found that there existed characterized absorption of –OH at 3,300 cm^{-1} in the PA and PSi membranes. So, this showed that PA and PSi membranes had obvious hydrophilic properties.

3.2. Morphology of blend membranes

Fig. 4 shows the cross-sectional SEM images of P, PA, PSi, and PS membranes, and the arrows in the figure refer to the top surface of the membranes. Compared with the original P membrane, it can be seen that the cross-sectional macropores of the modified membrane increased, and the structure support layer became loose gradually, this kind of structure was beneficial to the increase of the flux. Particularly, for the PA membrane, the spongy structure was emerged in the sub-layer, which is associated with the hydrophilicity of PVA itself and the influence of PVA on film-forming process [18].

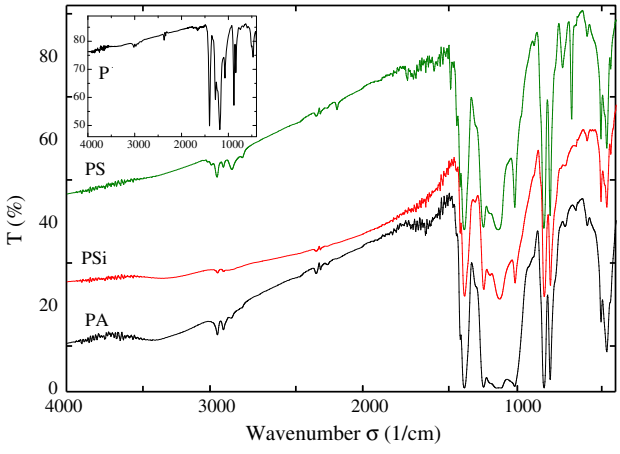

Fig. 3. FT-IR spectra of PA, PS and PSi membrane.

Fig. 5 shows the AFM images of P, PA, PSi, and PS membranes. It can be seen from Fig. 5 that, compared with the original P membrane, the membrane surface roughness of the modified membrane increased, but the values of Ra were relatively close. The main reason of this kind of rough behavior was that thermodynamic properties of the casting solution became unstable to a certain extent because of the introduction of additives. Thus, the film-forming process of the PVDF UF membrane was changed.

3.3. Properties of different PVDF UF membranes

Table 2 shows the structure parameters and performance data of the P, PA, PS, and PSi membranes. It can be seen from Table 2 that, compared with the P membrane, the WCA, *S*, and FBP of three modified films decreased, and the SI and J_p increased. Meanwhile, it can be also found that, compared with the PS membrane, the above-mentioned properties of the PA and PSi films changed more obviously. This indicates that the membrane structure parameters and hydrophilicity of the PVDF UF membrane were largely improved. Furthermore, attention should be paid to the fact that the data of porosity and pore size of the PA and PSi films might be larger than the actual value. The reason might have something to do with the above-mentioned improvement of the hydrophilicity. On the whole, it coincided with the SEM structure analysis, WCA, and swelling index of the membranes.

3.4. Antifouling behavior of modified membranes

Table 3 shows the static adsorption, rejection, and FR after continuous filtration to RB5 and CR of four PVDF UF membranes. Compared with the original P membrane, the data in the table show that the static adsorption amount to dyes of three membranes all reduced, but the rejection and FR rate to dyes increased. Particularly, the static adsorption and flux of PA and PSi films to CR and RB5 showed a more outstanding performance. And the reason may be

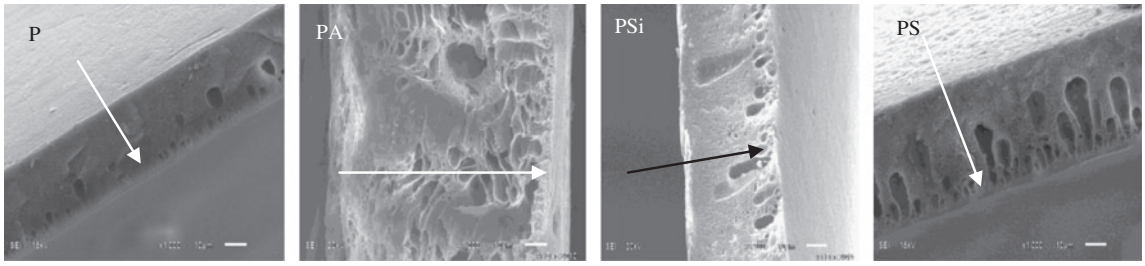

Fig. 4. SEM images of a PVDF blend UF membrane (1,000×).

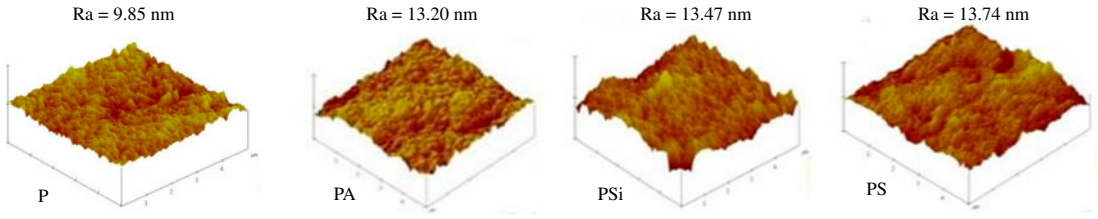

Fig. 5. AFM images of PVDF blend UF membranes.

Table 2
Properties of different PVDF UF membranes

Membrane number	r_m (nm)	ε (%)	SI (%)	WCA (°)	J_p (L m^{-2} h^{-1})	S (MPa)	FBP (MPa)
P	3.61	67.07	1.21	82.67	14.33	4.90	0.47
PA	5.16	87	3.47	58	56	3.52	0.35
PS	3.67	62	1.42	73	25.2	4.75	0.45
PSi	4.28	79.5	1.56	65	48	4.35	0.42

Table 3
The adsorption and rejection to CR and RB5 of different PVDF UF membranes

Membrane	Q_{CR} (mg/cm^2)	R_{CR} (%)	Q_{RB} (mg/cm^2)	R_{RB} (%)	FR (%)
P	0.363	61.4	0.412	65.5	69.0
PA	0.139	92.10	0. 205	91.2	98.4
PS	0.250	95.35	0. 375	96.0	88.6
PSi	0.086	96.56	0. 175	97.2	94.2

related to the fact that PA and PSi films had high hydrophilicity. Meanwhile, the concave and convex structure on the rough surfaces was not conducive to the deposition and adsorption of dye molecules on the surface of the membrane [19]. Therefore, the filtration experiment showed that the modified membrane had a good treatment effect on RB and CR dyes.

Fig. 6 shows diagrams of a continuous filtration of dyes for the four film fluxes. In this diagram, the water flux attenuation of the P membrane was the most severe. That means that the original P membrane was easily contaminated. On the contrast, the flux of the PS and PSi membranes was very stable. Hence, the fouling speed of the PS and PSi membranes was lower compared to the P membrane. Additionally, attention should be paid to the fact that the flux attenuation behavior of the PA membrane may be associated with the membrane structure [20]. But in continuous filtration, PA and PSi membranes all kept a good cleaning recovery rate. It is suggested that these two kinds of membrane fouling behaviors were reversible, and this may have resulted from the fact that for the PA and PSi membranes hydrophilicity and rough behavior at the membrane surface can prevent the adsorption of foulants on the membrane surface (see data in Table 3). Besides, three kinds of the modified membranes all had a great water production rate, so this has an important significance in the process of production.

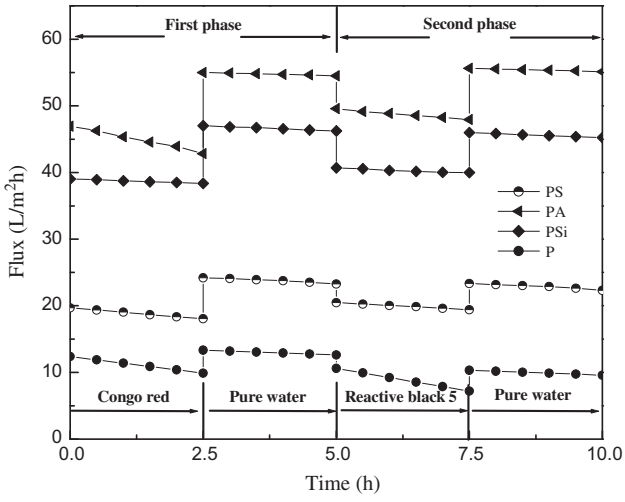

Fig. 6. Flux attenuation of PVDF UF membranes using RB5 and CR dye solutions.

4. Conclusions

Taking CR and RB5 as representatives, the filtration process and membrane behavior to foulants were investigated by three different types of modified PVDF UF membranes and the original PVDF membrane. Results showed that with the introduction of three kinds of additives, the membrane surface roughness increased, and the membrane hydrophilicity improved to a certain extent (WCA was lower than 73°). Meanwhile, the mechanical properties of the membrane reduced to different degrees. Although the FBP and *S* fall off to different degrees, FBP and *S* were still higher than 0.35 MPa and 3.52 MPa, respectively. However, the membrane performance and structure parameters were improved. The porosity of the membrane was greater than 79%, and the average pore size increased, >3.67 nm. Meanwhile, the penetration of the modified membrane was enhanced, the flux of pure water was more than 25.2 $L\,m^{-2}\,h^{-1}$. Owing to the introduction of PVA and SiO_2, the hydrophilicity of PVDF UF membrane was effectively improved. The adsorption of PA and PSi membranes which had great hydrophilicity to two dyes decreased, and the amount of static adsorption was lower than 0.375 g/m^2. FR rate was extremely high. And the cleaning recovery rate of PA and PSi was greater than 94.2%. Rejection of these two membranes to RB5 and CR maintained good rates, >91%, that is to say, PA and PSi the flux in the filtration of dyes were stable, and water yield was large. Consequently, it showed good anti-fouling properties and practical application value.

Acknowledgements

This research was financially supported by the National Natural Science Foundation of China (Grant No. 51008243, No. 51178378, No. 51278408), and the Ph.D. Programs Foundation of Ministry of Education of Education of China (Grant No. 20096120110010), and the Shaanxi Province and Science technology innovation project (Grant No. 2012KTCL03-06), and the 2011 Yulin Municipal Science and Technology Project.

References

[1] A. Akbari, J.C. Remigy, P. Aptel, Treatment of textile dye effluent using a polyamide-based nanofiltration membrane, Chem. Eng. Process 41 (2002) 601–609.
[2] C. Tang, V. Chen, Nanofiltration of textile wastewater for water reuse, Desalination 143 (2002) 11–20.
[3] M. Marcucci, G. Nosenzo, G. Capannelli, I. Ciabatti, D. Corrieri, G. Ciardelli, Treatment and reuse of textile effluents based on new ultrafiltration and other membrane technologies, Desalination 138 (2000) 75–82.
[4] C. Allègre, P. Moulin, M. Maisseu, F. Charbit, Treatment and reuse of reactive dyeing effluents, J. Membr. Sci. 269 (2006) 15–34.
[5] B. Kwon, J. Molek, A.L. Zydney, Ultrafiltration of PEGylated proteins: Fouling and concentration polarization effects, J. Membr. Sci. 319 (2008) 206–213.
[6] H.P. Srivastava, G. Arthanareeswaran, N. Ananthanthan, V.M. Starov, Performance of modified poly (vinylidene fluoride) membrane for textile wastewater ultrafiltration, Desalination 282 (2011) 87–94.
[7] R.M. Ribeiro, R. Bergamasco, M.L. Gimenes, Membranes synthesis study for colour removal of textile effluent, Desalination 145 (2002) 61–63.
[8] R. Han, Sh Zhang, Desalination of dye utilizing copoly (phthalazinone biphenyl ether sulfone) ultrafiltration membrane with low molecular weight cut-off, J. Membr. Sci. 358 (2010) 1–6.
[9] N. Bolong, A.F. Ismail, M.R. Salim, D. Rana, T. Matsuura, Development and characterization of novel charged surface modification macromolecule to polyethersulfone hollow fiber membrane with polyvinylpyrrolidone and water, J. Membr. Sci. 331 (2009) 40–49.
[10] R. Ahmad, S.M. Sayed, M. Yaghoub, Nano-porous polyethersulfone (PES) membranes modified by acrylic acid (AA) and 2-hydroxyethylmethacrylate (HEMA) as additives in the gelation media, J. Membr. Sci. 364 (2010) 380–388.
[11] W. Chinpa, D. Quémener, E. Bèche, R. Jiraratananon, A. Deratani, Preparation of poly (etherimide) based ultrafiltration membrane with low fouling property by surface modification with poly (ethylene glycol), J. Membr. Sci. 365 (2010) 89–97.
[12] A. Rahimpour, S.S. Madaeni, Y. Mansourpanah, Nano-porous polyethersulfone (PES) membranes modified by acrylic acid (AA) and 2-hydroxyethylmethacrylate (HEMA) as additives in the gelation media, J. Membr. Sci. 364 (2010) 380–388.
[13] H. Susanto, M. Ulbricht, Characteristics, performance and stability of polyethersulfone ultrafiltration membranes prepared by phase separation method

using different macromolecular additive, J. Membr. Sci. 327 (2009) 125–135.
[14] N. Li, C. Xiao, S. An, X. Hu, Preparation and properties of PVDF/PVA hollow fiber membranes, Desalination 250 (2010) 530–537.
[15] Q.-Z. Zheng, P. Wang, Y.-N. Yang, D.-J. Cui, The relationship between porosity and kinetics parameter of membrane formation in PSF ultrafiltration membrane, J. Membr. Sci. 286 (2006) 7–11.
[16] C. Feng, B. Shi, G. Li, Y. Wu, Preparation and properties of microporous membrane from poly(vinylidene fluoride-co-tetrafluoroethylene) (F2.4) for membrane distillation, J. Membr. Sci. 237 (2004) 15–24.
[17] A. Hernfindez, J.I. Calvo, P. Prfidanos, F. Tejerina, Pore size distributions in microporous membranes. A critical analysis of the bubble point extended method, J. Membr. Sci. 112 (1996) 1–12.
[18] X.-r. Meng, L. Zhao, L. Wang, X.-D. Wang, D.-X. Huang, R. Miao, Study of antifouling modified ultrafiltration membrane based on the secondary treated water of urban sewage, Water Sci. Technol. 66 (2012) 2074–2082.
[19] P. Wang, Z. Wang, Z. Wu, S. Mai, Fouling behaviours of two membranes in a submerged membrane bioreactor for municipal wastewater treatment, J. Membr. Sci. 382 (2011) 60–69.
[20] M. Hirose, H. Ito, Y. Kamiyama, Effect of skin layer surface structures on the flux behavior of RO membranes, J. Membr. Sci. 121 (1996) 209–215.